(2), 30–37 kcal mol^{-1} for 1,2-dihydroazete (3), and 37 kcal mol^{-1} for 3,4-dihydroazete (4). Two diastereomeric pathways are allowed for the opening of 1 and 3. The favored pathway involves the heteroatom lone pair rotating inward. This rotation allows for stabilization of the C–P or C–N σ^* orbital through overlap with the lone pair and thereby stabilizes the TS. Experimental verification of these results awaits the synthesis of stable dihydrophosphetes with pendent groups that can stabilize the product phosphabutadiene.

Acknowledgment is made to the Donors of the Petroleum Research Fund, administered by the American Chemical Society, for support of this research and to the National Science Foundation for equipment grant DIR-8907135.

Registry No. 1, 132515-09-4; 2, 125033-70-7; 3, 6788-71-2; 4, 6788-85-8; 11, 137465-59-9; 12, 137465-60-2; 13, 122682-85-3; 14, 73311-40-7; 15, 80861-03-6; 16, 38239-27-9.

Supplementary Material Available: Optimized geometries in the form of Z matrices for all structures at the HF/6-31G* and MP2/6-31G* levels (10 pages). This material is contained in many libraries on microfiche, immediately follows this article in the microfilm version of the journal, and can be ordered from the ACS; see any current masthead page for ordering information.

Incipient Nucleophilic Attack as a Probe for the Electronic Structure of Diazonium Ions. An Analysis of Neighboring-Group Interactions in β-(Carboxyvinyl)diazonium Ions

Rainer Glaser,* Christopher J. Horan,[1] Eric D. Nelson, and M. Kirk Hall

Department of Chemistry, University of Missouri, Columbia, Missouri 65211

Received July 15, 1991

Crystal structures of diazonium ions with nucleophilic neighboring groups exhibit distortions that have commonly been interpreted by postulating an "incipient nucleophilic attack" of the proximate nucleophile on N_α. We have recently challenged the assumption that the charge distribution is correctly represented by the most important Lewis structure R—N$^+$≡N and propose here an alternative explanation of these structural features thereby providing a crucial link between the theoretically derived bonding model and experimental data. The rotamers of 3-diazonium propenoic acid and their zwitterions are examined in this context. The role of the atomic first moments for a correct appreciation of the anisotropy of the electron density distribution within the atomic basins and for an adequate description of electrostatic interaction between neighboring groups is discussed. A method is described for the evaluation of neighboring group interactions based on integrated atomic charges, first moments and quadrupole moments. It is found that the electrostatic interactions of the neighboring groups in the cis isomers correlate with the nucleophilicity of the proximate nucleophile and that the differences in the neighboring group interactions of geometrical isomers correlate with the cis preference energies.

Introduction

Diazonium ions are important reactive intermediates, and several resonance forms have been employed to discuss a variety of their properties.[2] The most popular resonance from—and the one commonly found in textbooks—is the resonance form A (Chart I) in which N_α is *formally* assigned a positive charge. The resonance form B may be conveniently used to explain azo coupling and like reactions in which N_β acts as the electrophilic center. While the resonance forms A and B usually are considered to suffice for the description of aliphatic diazonium ions, several others are discussed additionally for aromatic diazonium ions. The various resonance forms that result from π-electron pair pushing from the phenyl ring to the N_2 group are collectively referred to as resonance forms C_{Ar} in the scheme. The resonance form D_{Ar} resembles A but takes into account a polarization of the π density of the ring and D_{Ar} has been regarded as a major contributor to the ground-state electronic structure.[3,4]

Chart I

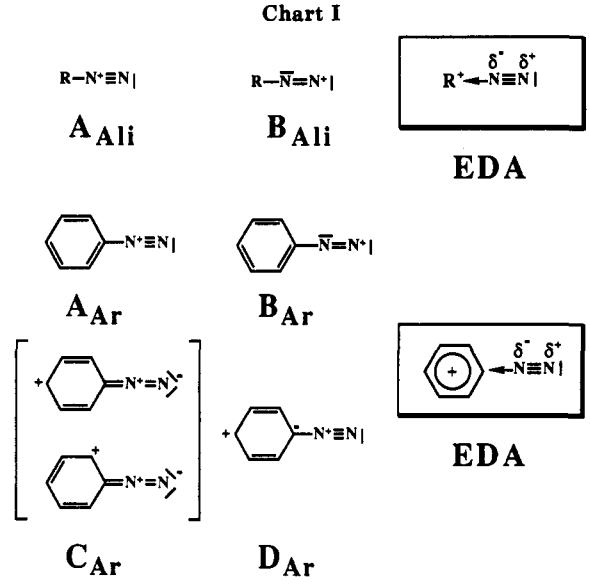

These resonance forms either assign a formal positive charge to the N_2 group (A, B, D) or none (C), and, with the exception of B, they assign the formal positive charge to N_α. Considering the qualitative rules regarding the relative contributions of the resonance forms, the resonance form A (and D) is appropriate indeed for the description of the diazonium ions. We have recently shown however that the *formal* charges of these resonance forms

(1) (a) Part of the projected dissertation of Christopher J. Horan. (b) Presented in part at the 25th ACS Midwest Regional Meeting, Manhattan, KS, Nov 8, 1990 and at the American Chemical Society National Meeting, Atlanta, GA, April 14, 1991.

(2) For reviews on diazonium ions, see: (a) Zollinger, H. *Acc. Chem. Res.* **1973**, *6*, 335. (b) Zollinger, H. *Azo and Diazo Chemistry*; Wiley Interscience, New York, 1961. (c) Patai, S., Ed. *The Chemistry of the Diazonium and Diazo Groups*; Wiley Interscience, New York, 1978. (d) Laali, K., Olah, G. A. *Rev. Chem. Intermed.* **1985**, *6*, 237.

(3) Elofson, R. M.; Cyr, N.; Laidler, J. K.; Schulz, K. F.; Gadallah, F. F. *Can. J. Chem.* **1984**, *62*, 92.

(4) Olah, G. A.; Grant, J. L. *J. Am. Chem. Soc.* **1975**, *97*, 1546.

0022-3263/92/1957-0215$03.00/0

Chart II

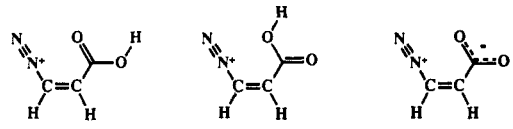

1 2 4

do not provide good representations of the *actual* charge distribution.[5,6] Electron density analysis (EDA) of prototypical aliphatic diazonium ions at the RHF/6-31G* level has revealed that the overall charge of the N_2 group is rather small (<+0.16). The charge transfer from N_2 to the hydrocarbon fragment remains small even in dications such as cyclopropeniumyldiazonium dications,[7,8] and electron density analyses of the correlated electron density functions of methyl- and ethyldiazonium ions[9] have confirmed this new bonding model. In all cases, the electron density distribution within the N_2 group is characterized by a strong polarization of the type $^{\delta-}N_\alpha-N_\beta{}^{\delta+}$. While the direction of this internal polarization is consistent with the large positive charge on the hydrocarbon fragment, it is opposite to what would be expected based on qualitative considerations of resonance forms. Both of the features identified as typical for the aliphatic diazonium ions, small N_2 charge and strong internal N_2 polarization, also are found in the phenyldiazonium ion.[10]

In the present study, we are using the "incipient nucleophilic attack" as a probe for the electronic structure of diazonium ions to test and to corroborate our bonding model. Crystal structure databases were searched for diazonium ions that contain a proximate nucleophile. Features of such crystal structures that had been explained by an incipient nucleophilic attack at N_α were analyzed for their consistency with the new bonding model. The theoretical studies reported here focus on an analysis of neighboring group interactions in the rotamers of 3-diazonium propenoic acid, **1** and **2**, and the corresponding zwitterion **4**. These propenoic acid derivatives are particularly suitable for our purpose. First, the three systems allow for a variation of the nucleophilicity of the O atom in the proximity of the N_2 group without major skeleton changes. Second, an aliphatic unsaturated molecule was selected because it allows for a study of the incipient nucleophilic attack in the CC cis-configured geometrical isomer in comparison to the trans isomers. This comparison is important to dissect the effects of the incipient nucleophilic attack from others.

Methodological Aspects

Nomenclature. The isomers of 3-diazonium propenoic acid in which the carbonyl O and C_α are s-cis or s-trans with regard to the CC single bond are referred to as **1** and **2**, respectively, and **3** are the associated rotational transition-state structures. The planar 3-diazonium propenoate zwitterions are referred to as **4**, and **5** are the transition-state structures for the narcissistic automerizations of **4**. Geometrical isomers are identified by a or b if the functional groups are cis or trans with regard to the C=C bond, respectively.

Chart III

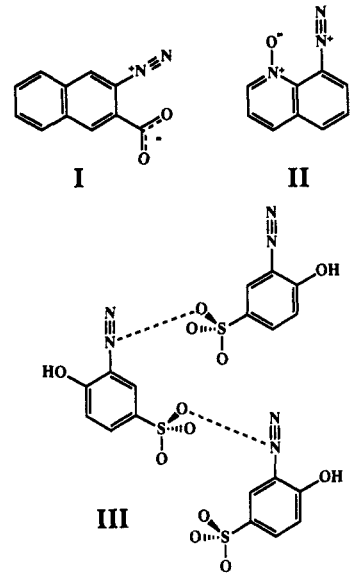

I II III

Ab Initio Computations. Geometries were optimized with the gradient algorithms of either Schlegel or Baker using both GAUSSIAN88[11] and GAMESS.[12] C_s symmetry was imposed on **1**, **2**, **4**, and **5**. The Hessian matrices were computed analytically for each of the structures to confirm that an extremum had indeed been located, to characterize the stationary structures via the number of negative eigenvalues, and to determine the harmonic vibrational frequencies and the vibrational zero-point energies (VZPEs). VZPE corrections to relative energies have to be scaled by the usual factor of 0.9 to account for the typical overestimation at this level.[13] Geometry optimizations and normal-mode analyses were carried out at the restricted Hartree–Fock (RHF) level with the 3-21G basis set, and the structures were subsequently reoptimized with the 6-31G* basis set.[14] To assure a sufficiently flexible AO basis for "anionic parts" of the zwitterions, all computations of **4** and **5** were carried out with additional shells of diffuse functions on all heavy atoms (3-21+G and 6-31+G*) but they were found to be not important in these neutral molecules. Electron correlation effects on energies were estimated using Møller–Plesset[15] perturbation theory to second and third order in the frozen core approximation with the RHF/6-31G* or RHF/6-31+G* structures, re-

(5) Glaser, R. *J. Phys. Chem.* **1989**, *93*, 7993.

(6) The charge on N_α in the best VB structure is a formal charge that is obtained merely through a bookkeeping procedure. It is not intended to be the actual charge of the atom. Carbon monoxide provides a well-known example for a molecule in which the formal charges of the best resonance structure provide a poor indication of the actual charge distribution. We thank one of the reviewers for pointing out this example.

(7) Glaser, R. *J. Comput. Chem.* **1990**, *11*, 663.

(8) Significant charge transfer occurs only in heterosubstituted diazonium ions, XN_2^+ (X = F, OH, NH_2): Glaser, R.; Choy, G. S.-C. *J. Phys. Chem.*, in press.

(9) Glaser, R.; Choy, G. S.-C.; Hall, M. K. *J. Am. Chem. Soc.* **1991**, *113*, 1109.

(10) Glaser, R.; Horan, C. J. To be published. The major difference between the aliphatic and aromatic diazonium ions occurs in the hydrocarbon fragment; the positive charge is delocalized over the entire phenyl ring in the phenyldiazonium ion.

(11) GAUSSIAN88 (Rev. C): Frisch, M. J.; Head-Gordon, M.; Schlegel, H. B.; Raghavachari, K.; Binkley, J. S.; Gonzales, C.; DeFrees, D. J.; Fox, D. J.; Whiteside, R. A.; Seeger, R.; Melius, C. F.; Baker, J.; Martin, R. L.; Kahn, L. R.; Stewart, J. J. P.; Fluder, E. M.; Topiol, S.; Pople, J. A. Gaussian, Inc., Pittsburgh, PA, 1988.

(12) GAMESS: Schmidt, M. W.; Boatz, J. A.; Baldridge, K. K.; Koseki, S.; Gordon, M. S.; Elbert, S. T.; Lam, B. QCPE **1987**, *7*, 115.

(13) Hehre, W. J.; Radom, L.; Schleyer, P. v. R.; Pople, J. A. *Ab Initio Molecular Orbital Theory*; John Wiley & Sons, New York, 1986.

(14) (a) Hehre, W. J.; Ditchfield, R.; Pople, J. A. *J. Chem. Phys.* **1972**, *56*, 2257. (b) Hariharan, P. C.; Pople, J. A. *Theor. Chim. Acta* **1973**, *28*, 213. (c) Binkley, J. S.; Gordon, M. S.; DeFrees, D. J.; Pople, J. A. *J. Chem. Phys.* **1982**, *77*, 3654. (d) Six Cartesian second-order Gaussians were used for d shells.

(15) (a) Møller, C.; Plesset, M. S. *Phys. Rev.* **1934**, *46*, 1243. (b) Binkley, J. S.; Pople, J. A. *Int. J. Quantum Chem.* **1975**, *9*, 229. (c) Pople, J.A.; Seeger, R. *Int. J. Quantum Chem.* **1976**, *10*, 1. (d) Pople J. A.; Krishnan, R.; Schlegel, H. B.; Binkley, J. S. *Int. J. Quantum Chem.* **1978**, *14*, 91.

spectively, with the same basis sets. The diazonium propenoates might be viewed as arising from the corresponding heterocycle via either heterolytical or homolytical bond cleavage and diradical contributions might thus be important for their correct description. The stability of the RHF/6-31+G* wave function of **4a** was tested[16] with regard to relaxation of the RHF constraints and it was found to be stable.

Electron Density Analysis. Topological and integrated properties[17,18] of the electron densities and gradient vector fields were determined with Bader's programs EXTREME, PROAIM, and SCHUSS.[19] Cross sections and three-dimensional matrices of $\rho(x,y,z)$ were determined with the program[20] NETZ3D, and PV-WAVE programs were written for their graphical display. Three-dimensional contour plots of electron density matrices computed with NETZ3D were produced with Jorgensen's programs[21] PSICON and PSI2. The programs DIPOLES[20] and ESI[22] were written to analyze properties of the integrated atomic moments.

Crystal Structures of Diazonium Ions

In crystal structures[23] of diazonium ions that contain a proximate nucleophile (Chart III), it has been found that the N_2 group is bent in a way that suggested an incipient attack of that nucleophile on N_α of N_2.[24-27] Gougoutas et al. attributed the distortions in 3-carboxy-2-naphthalenediazonium salts[24] to an attractive interaction between N_α and the carbonyl O and between N_β and the gegenion. An even shorter approach of the carbonyl O toward N_α was found in the 3-carboxylato-2-naphthalenediazonium zwitterion I.[25] Wallis and Dunitz[26] explained the distortions in the crystal structure of quinoline-8-diazonium 1-oxide tetrafluoroborate II in the same way. These explanations assume that the *formal* N_α charge in the Lewis structure well represents the *actual* charge distribution. Our recently proposed bonding model, however, suggests that these distortions actually are the result of optimal approach of the nucleophile toward the positively charged *C atom* to which the diazo group is attached and that this approach occurs *despite* the repulsive interactions between the negatively charged N_α and the proximate nucleophile. In both the crystal structures of the 3-carboxylato-2-naphthalenediazonium salts and zwitterions and of II, the N_2 group and the nucleophile are placed on *opposite* sides of the best plane of the molecules; this feature only is accounted for by the explanation offered by our model.[5] A similar *inter*molecular incipient nucleophilic attack of the sulfonate O on the N_α atom of a neighboring molecule has been discussed for the structure of 1-hydroxy-4-sulfonatobenzene-2-diazonium monohydrate, III, reported by Greenberg and Okaya.[28] The close O–N_α contact might, however, equally well be explained as *a consequence* of minimization of the distances between the sulfonate O and N_β and the C atom to which the diazonium group is attached, rather than *the cause* for the short $(SO_2)ON_\alpha$ distance. The placement of nucleophiles in such 1,3-*bridging* positions appears to be a common structural concept. The structures are known of several diazonium ions with large polyfluoro gegenions in which the F atoms are placed successively in the two CNN bridging positions and, if both of these are occupied, in the proximity of the terminal nitrogen (Chart IV). The crystal structures of *p*-bromobenzene tetrafluoroborate,[29] IV, determined by Sasvari et al. as well as that of *p*-(di-

Chart IV

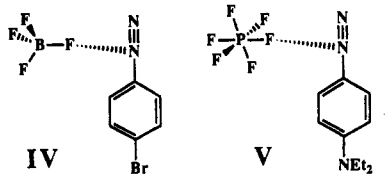

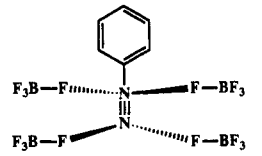

VI

Table I. Cis Preference Energies, Conformational Preference Energies, and Activation Barriers[a]

	3-21G		/6-31G*//RHF/6-31G*		
	ΔVZPE	RHF	RHF	MP2	MP3
Cis Preference Energies					
1b vs 1a	−0.20	2.40	2.82	3.27	3.16
2b vs 2a	−0.31	0.54	0.03	0.80	0.64
4b vs 4a	−0.47	9.09	8.31[b]	8.73	9.13
Conformational Preference Energies					
2a vs 1a	0.05	1.88	3.77	3.69	3.56
2b vs 1b	−0.05	0.01	0.97	1.22	1.05
Activation Barriers					
3a vs 1a	−0.69	11.25			
3a vs 2a	−0.75	9.37			
3b vs 1b	−0.66	9.19	4.77	4.78	4.74
3b vs 2b	−0.60	9.17	3.80	3.56	3.92
5a vs 4a	−0.68	7.27	4.12	3.38	4.59
5b vs 4b	−0.57	4.70	0.91	−1.28	0.78
Proton Affinities					
4a vs 1a	−8.81	204.50	238.54	221.41	237.62
4b vs 1b	−8.61	211.19	244.04	226.87	234.47

[a] All values are in kcal/mol. Total energies and vibrational zero-point energies are given as supplementary material. [b] The energies of **4a** and **4b** at RHF/6-31G*//RHF/6-31+G* are −373.274 57 and −373.261 27 atomic units, and the relative energy is 8.34 kcal/mol.

(16) Seeger, R.; Pople, J. A. *J. Chem. Phys.* **1977**, *66*, 7.
(17) Bader, R. F. W. *Atoms in Molecules—A Quantum Theory*; Clarendon Press: Oxford University Press, Oxford, OX2 6DP, U.K., 1990.
(18) For reviews, see for example: (a) Bader, R. F. W. *Acc. Chem. Res.* **1985**, *18*, 9. (b) Bader, R. F. W.; Nguyen-Dang, T. T.; Tal, Y. *Rep. Prog. Phys.* **1981**, *44*, 893. (c) Glaser, R. *J. Comput. Chem.* **1989**, *10*, 118.
(19) (a) Biegler-Koenig, F. W.; Bader, R. F. W.; Tang, T. H. *J. Comput. Chem.* **1982**, *3*, 317. (b) EXTREME and PROAIM were ported both to the IBM 4381 by G. Choy and to the Silicon Graphics Personal Iris by R. Glaser.
(20) Programs NETZ3D and DIPOLES were written by Glaser, R., Department of Chemistry, University of Missouri—Columbia, 1990.
(21) PSICON and PSI2 written by: Severance, D. L.; Jorgensen, W. L. Department of Chemistry, Purdue University, West Lafayette, IN.
(22) Program ESI (Version 1.2) written by: Glaser, R.; Hall, M. K. Department of Chemistry, University of Missouri—Columbia, 1991.
(23) The Cambridge Structural Database and the associated software systems (Version 4.2) were used for crystal structure searches. Cambridge Crystallographic Data Centre, University Chemical Laboratory, Lensfield Road, Cambridge CB2 1EW, U.K.
(24) 3-Carboxy-2-naphthalenediazonium salts: (a) Bromide, chloride, and bisulfate: Gougoutas, J. Z.; Johnson, J. *J. Am. Chem. Soc.* **1978**, *100*, 5816. (b) Iodide: Gougoutas, J. Z. *J. Am. Chem. Soc.* **1979**, *101*, 5672.
(25) 3-Carboxy-2-naphthalenediazonium zwitterion: Gougoutas, J. Z. *Cryst. Struct. Commun.* **1982**, *11*, 1305.
(26) Quinoline-8-diazonium 1-oxide tetrafluoroborate: Wallis, J. D.; Dunitz, J. D. *J. Chem. Soc., Chem. Commun.* **1984**, 671.
(27) 2-(Dimethylamino)benzenediazonium cation: Wallis, J. D.; Dunitz, J. D. *Helv. Chim. Acta* **1984**, *67*, 1374.
(28) 2-Diazonium 4-phenolsulfonate monohydrate: Greenberg, B.; Okaya, Y. *Acta Crystallogr.* **1969**, *B25*, 2101.
(29) *p*-Bromobenzene tetrafluoroborate: Sasvari, K.; Hess, H.; Schwarz, W. *Cryst. Struct. Commun.* **1982**, *11*, 781.

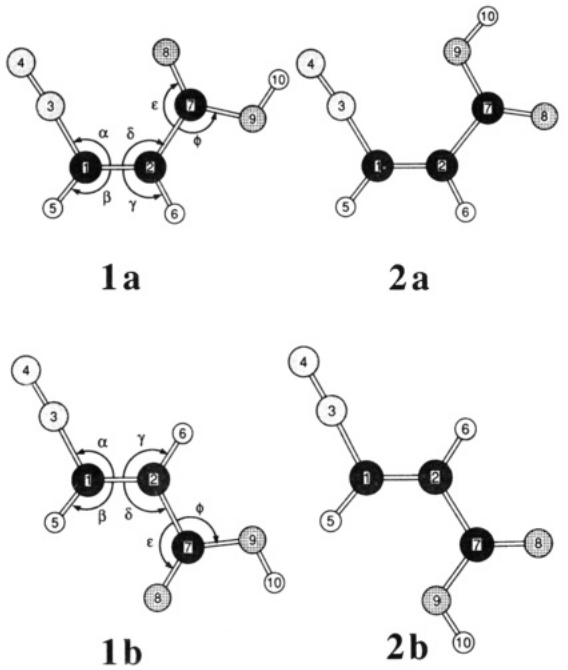

Figure 1. RHF/6-31G* optimized geometries of the rotamers **1a** and **2a** of the C(1)C(2) *cis*-configured 3-diazonium propenoic acid and of their trans isomers **1b** and **2b**.

ethylamino)benzenediazonium hexafluorophosphate,[30] V, reported by Ball et al. both have F atoms in such bridging positions with nearly identical F–N_α and F–N_β distances. The crystal structure of benzenediazonium tetrafluoroborate,[31] VI, determined by Cyler et al. provides an excellent example of the latter. The positions of the bridging fluorines with regard to the N_2 group have been regarded as the result of electrostatic interactions between N_α (and N_β) and these fluorines but they are equally compatible and perhaps better explained by our model.

Results and Discussion

Potential Energy Surface Analysis. Cis preference energies, conformational preference energies and activation barriers are summarized in Table I. Structural parameters are documented in Tables II and III.

3-Diazonium Propenoic Acid Isomers. Drawings of the planar RHF/6-31G* optimized structures of the rotamers of the cis and the trans configured 3-diazonium propenoic acid are depicted in Figure 1. All of these structures were shown to be minima by analytical computation of the Hessian matrix at the RHF/3-21G level.

Conformational Preference. In the cis configuration, a thermodynamic preference is found for that conformation in which the carbonyl O is directed toward the N_2 group (**1a** is more stable than **2a**). The conformational preference energy is 1.88 kcal/mol at the RHF/3-21G level, and it is increased to 3.77 kcal/mol at the RHF/6-31G* level. In the trans configuration, the conformational preference is drastically reduced. While **1b** and **2b** are essentially isoenergetic at RHF/3-21G, there is a small preference of 0.97 kcal/mol for **1b** over **2b** at the RHF/6-31G* level. Electron correlation affects the conformational preference energies only slightly. At our best level and including (scaled) vibrational zero-point energy differences, **1a** and **1b** are preferred over **2a** and **2b** by 3.61 and 1.00 kcal/mol, respectively. It is thus more favorable to have the carbonyl O close to the N_2 group than the hydroxyl oxygen, and this preference is more pronounced in the cis than in the trans configuration.

Rotational Transition States. At the RHF/3-21G level, a significant activation barrier is found for the isomerization between **1a** and **2a**; **3a** is 11.25 and 9.37 kcal/mol less stable than **1a** and **2a**, respectively. Reoptimization of **3a** at the RHF/6-31G* level, however, leads to a transition-state structure that is very similar to **2a** with only a slight rotation of the carboxyl group out of the plane. The exact location of **3a** on the RHF/6-31G* surface was not determined. Instead, to corroborate the flatness of the potential energy surface around **2a**, we determined vibrational frequencies for **2a** also at the 6-31G* level. The frequency of the normal mode associated with the carboxyl rotation in **2a** is 47 cm^{-1}; this frequency

Table II. Structures of 3-Diazonium Propenoic Acid[a]

	CC cis configuration				
	1a		**2a**		**3a**
parameters	3-21G	6-31G*	3-21G	6-31G*	3-21G
C1–C2	1.314	1.318	1.315	1.320	1.315
C1–N3	1.437	1.434	1.428	1.431	1.438
N3–N4	1.079	1.074	1.079	1.074	1.081
C1–H5	1.068	1.071	1.068	1.071	1.067
C2–H6	1.070	1.074	1.071	1.075	1.074
C2–C7	1.498	1.509	1.492	1.507	1.506
C7–O8	1.200	1.183	1.191	1.173	1.191
C7–O9	1.321	1.300	1.344	1.320	1.334
O9–H10	0.972	0.957	0.972	0.958	0.973
C2–C1–N3	120.37	120.06	122.18	121.20	119.54
C1–N3–N4	181.79	184.49	182.17	184.41	181.98
H5–C1–C2	128.32	128.95	126.91	128.14	128.93
H6–C2–C1	119.23	117.51	117.64	116.50	117.45
C7–C2–C1	122.60	123.54	126.96	129.02	125.29
O8–C7–C2	122.36	121.46	122.51	120.52	124.13
O9–C7–C2	110.18	110.86	111.20	112.54	108.29
H10–O9–C7	115.84	111.31	114.31	110.40	115.31
H6–C2–C1–H5	0.00	0.00	0.00	0.00	0.00
C7–C2–C1–H5	180.00	180.00	180.00	180.00	179.00
N3–C1–C2–H6	180.00	180.00	180.00	180.00	180.00
O8–C7–C2–C1	0.00	0.00	180.00	180.00	–92.08
O9–C7–C2–C1	180.00	180.00	0.00	0.00	87.66
H10–O9–C7–C2	180.00	180.00	180.00	180.00	173.43

	CC trans configuration					
	1b		**2b**		**3b**	
parameters	3-21G	6-31G*	3-21G	6-31G*	3-21G	6-31G*
C1–C2	1.315	1.319	1.315	1.320	1.315	1.319
C1–N3	1.427	1.429	1.435	1.432	1.436	1.429
N3–N4	1.081	1.076	1.081	1.076	1.081	1.076
C1–H5	1.070	1.072	1.068	1.071	1.068	1.071
C2–H6	1.070	1.075	1.071	1.075	1.074	1.076
C2–C7	1.504	1.515	1.497	1.509	1.510	1.515
C7–O8	1.196	1.179	1.192	1.175	1.190	1.174
C7–O9	1.326	1.305	1.339	1.314	1.332	1.307
O9–H10	0.972	0.957	0.971	0.957	0.972	0.958
C2–C1–N3	120.13	118.08	119.22	117.32	118.94	117.47
C1–N3–N4	181.77	182.39	181.77	182.08	181.68	182.17
H5–C1–C2	127.04	129.15	128.31	130.58	129.63	130.78
H6–C2–C1	125.71	123.70	124.72	123.20	122.85	122.17
C7–C2–C1	115.61	116.40	118.69	121.28	120.30	121.01
O8–C7–C2	122.34	121.28	122.53	120.49	123.77	120.54
O9–C7–C2	109.87	110.72	110.38	111.82	108.17	110.76
H10–O9–C7	115.49	111.02	115.26	110.76	115.25	110.87
H6–C2–C1–H5	180.00	180.00	180.00	180.00	179.68	179.77
C7–C2–C1–H5	0.00	0.00	0.00	0.00	–1.27	–2.77
N3–C1–C2–H6	0.00	0.00	0.00	0.00	–0.32	–0.31
O8–C7–C2–C1	0.00	0.00	180.00	180.00	–92.60	–91.67
O9–C7–C2–C1	180.00	180.00	0.00	0.00	88.34	89.36
H10–O9–C7–C2	180.00	180.00	180.00	180.00	176.64	177.32

[a] Bond lengths are in angstroms and angles are in degrees. [b] At RHF/6-31G*, vibrational frequency analysis shows **2a** to be a minimum.

(30) *p*-(Diethylamino)benzenediazonium hexafluorophosphate: Ball, R. G.; Elofson, R. M. *Can J. Chem.* **1985**, *63*, 332.

(31) Benzenediazonium tetrafluoroborate: Cygler, M.; Przybylska, M.; Elofson, R. M. *Can J. Chem.* **1982**, *60*, 2852.

Table III. Structures of the Cis and Trans Zwitterions of 3-Diazonium Propenoate[a]

	cis				trans			
	4a		5a		4b		5b	
parameters	3-21+G	6-31+G*	3-21+G	6-31+G*	3-21+G	6-31+G*	3-21+G	6-31+G*
C1–C2	1.321	1.325	1.329	1.335	1.327	1.332	1.333	1.340
C1–N3	1.447	1.429	1.437	1.413	1.428	1.411	1.419	1.396
N3–N4	1.081	1.075	1.084	1.077	1.086	1.079	1.087	1.081
C1–H5	1.067	1.069	1.067	1.069	1.071	1.070	1.068	1.070
C2–H6	1.072	1.075	1.073	1.075	1.073	1.077	1.075	1.077
C2–C7	1.563	1.567	1.552	1.554	1.578	1.580	1.563	1.555
C7–O8	1.235	1.209	1.244	1.216	1.239	1.214	1.241	1.214
C7–O9	1.257	1.229	1.244	1.216	1.248	1.219	1.241	1.214
C2–C1–N3	119.35	119.00	115.76	115.10	119.37	118.26	119.15	118.04
C1–N3–N4	185.77	188.86	180.32	180.63	181.67	180.95	181.60	180.55
H5–C1–C2	130.72	130.92	132.57	132.58	127.13	127.93	128.96	129.04
H6–C2–C1	118.59	116.99	118.65	117.32	124.77	122.34	122.36	120.61
C7–C2–C1	123.61	124.04	121.76	123.09	116.50	118.26	120.29	121.58
O8–C7–C2	112.35	112.03	112.57	111.92	112.73	112.37	112.12	111.50
O9–C7–C2	113.74	113.05	112.57	111.93	112.50	111.69	112.12	111.50
H6–C2–C1–H5	0.00	0.00	0.00	0.00	180.00	−179.68	180.00	180.00
C7–C2–C1–H5	180.00	180.00	180.00	180.00	0.00	0.00	0.00	0.00
N3–C1–C2–H6	180.00	180.00	180.00	180.00	0.00	0.00	0.00	0.00
O8–C7–C2–C1	0.00	0.00	88.36	88.87	0.00	0.00	90.30	90.33
O9–C7–C2–C1	180.00	180.00	−88.36	−88.86	180.00	180.00	−90.30	−90.34

[a] Bond lengths are in angstroms and angles are in degrees.

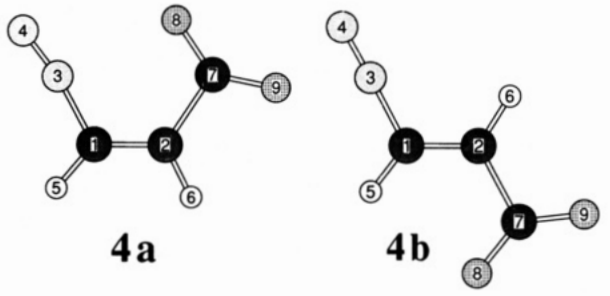

Figure 2. RHF/6-31+G* geometries of the C(1)C(2) cis- and trans-configured 3-diazonium propenoate zwitterions **4a** and **4b**, respectively.

is indeed rather low but **2a** corresponds to a local minimum at this level. Polarization functions thus reduce the activation barrier for the process **1a** to **2a**, and **3a** becomes energetically and structurally close to **2a**. For the trans isomers, basis set effects on the structure are less significant (Table II). At the RHF/6-31G* level, the activation energies for the interconversion of **1b** into **2b** and **2b** into **1b** are 4.77 and 3.80 kcal/mol, respectively, and they are smaller compared to the activation energies determined with the unpolarized basis set. Electron correlation has little effect, but the inclusion of zero-point energies reduces these barriers to 4.15 and 3.38 kcal/mol.

3-Diazonium Propenoate. The planar minima of the cis- and trans-configured zwitterions **4a** and **4b** are shown in Figure 2. The activation energies for the rotation of the carboxylate group via **5a** or **5b**, respectively, are 7.27 (cis) and 4.70 kcal/mol at RHF/3-21+G, and they are reduced to 4.12 (cis) and 0.91 kcal/mol at RHF/6-31+G*.[32] As with the acids, π interactions between the carboxyl group and the CC double bond are small.

Cis Preference Energies. A cis preference is found for all of the systems at both of the RHF levels. At the higher level, the cis preference energies are 2.82 (**1**), 0.03 (**2**), and 8.31 (**4**) kcal/mol and they reflect the nucleophilicity of the O atom in the proximity of the diazonium group. In our analysis of the origin of cis preference energies, we will be making use of atomic properties determined with the Hartree–Fock wave functions. The excellent linear correlations[33] between the RHF cis preference energies and the corresponding values determined at the correlated levels justify this approach.

Geometries and Electronic Structures. 3-Diazonium Propenoic Acid Isomers. In general, corresponding bond lengths in **1** and **2** differ only slightly. The NN bond lengths (1.074–1.076 Å) are the same, indicative of an NN triple bond, and slightly shorter than the NN bond length in free N_2 (1.097 Å). The CN bond distances are in the range 1.429–1.434 Å. Both of these bond lengths essentially are the same as those of the parent vinyldiazonium ion.[5] The C(1)=C(2) lengths also are confined to a rather narrow interval of 1.318–1.320 Å, and the C(2)–C(7) bonds are about 1.510 Å long with only a slightly longer bond of 1.515 Å in **1b**. These structural features suggest that there is little (if any) conjugation of the carboxyl π-system with the C(1)=C(2) bond.

Significant structural differences are found in the angles (see Figure 1 for definition). A typical feature common to all of the rotamers is the large deviation of the β angle from the sp^2 angle; the β angles (128.1–130.6°) are roughly 10° larger. The γ angles also differ from the standard sp^2 angle, but to a lesser extent and the deviations depend on the geometrical isomer. In cis **1a** and **2a**, the γ angles (117.5° and 116.5°) are reduced by about 3°, while they are increased by about the same amount in the trans isomers **2a** and **2b** (123.7° and 123.2°). A stronger dependency on the geometrical isomer is found for the δ angles. The δ angles of **1b** and **2b** are 116.4° and 121.3°, respectively, and the corresonding angles in the cis isomers **1a** and **2a** are 123.5° and 129.0°. The placement of the carboxyl group in the proximity of the N_2 group *increases* the δ angles by 7.1° (**1**) and 7.7° (**2**). This difference between the geometrical isomers is significant since the assumption of an attractive interaction between N_α and the proximate

(32) Note that the MP2 energies would indicate **5b** to be more stable than **4b**, but at the third-order perturbation level activation energies are obtained that are close to the RHF results.

(33) E(MP3) = 1.034 E(RHF) + 0.464 (R^2 = 0.998) and E(MP2) = 0.963 E(RHF) + 0.685 (R^2 = 0.999). The regression lines intersect the positive y axis indicating that the cis preference energies at the correlated levels are increased essentially by the same amount (0.69 (MP2) and 0.46 kcal/mol) for each of the molecules.

nucleophile in the cis isomer would suggest just the opposite. The α and the ϵ angles also affect the distances between the proximate nucleophile and N_α in the cis isomers. Both of these angles are increased in the cis structures compared to the trans structures, thereby *increasing* the N_α–O distance in the cis isomers even more. The α angles increase by 2° (**1b** to **1a**) and 4° (**2b** to **2a**), and the ϵ angles are increased but marginally. With regard to the absolute magnitude, a consistent difference between the ϵ and the ϕ angles is found: OCC angles involving a carbonyl O (ϵ) always are about 10° larger than are the OCC angles involving the hydroxyl O (ϕ), and it is the ϕ angles that deviate from the standard sp^2 angle.

3-Diazonium Propenoate Zwitterions. **4a** and **4b** show similar angular features and isomer dependencies as the cations. The β angles both are significantly larger than 120° (131.9° in **4a** and 127.9° in **4b**), the γ angle is smaller in the cis (117.0°) than in the trans isomer (122.3°), and the δ angle is significantly increased by 5.7° in **4a** (124.0°) compared to **4b** (118.3°). Both of the OCC angles are about 112–113° and they are close to the ϵ angles in the acids. The formation of the zwitterion has small effects on some of the bond lengths. While the NN bond lengths are affected little, the CN bond distance (1.411 Å) in trans **4b** is shortened significantly compared to the CN distances in the acids and also compared to cis **4a** (1.429 Å). The C(1)C(2) bonds are only slightly longer in the zwitterions but quite significant elongations of 0.06–0.07 Å of the C(2)C(7) bond lengths are found.

Atom and Fragment Populations. The RHF/6-31G* wave functions of **1**, **2**, and **4** were analyzed[34] topologically, and atom and fragment populations were determined via numerical integration within the atomic basins determined by the zero-flux surfaces of the electron density functions.[17,18] The zero-flux surfaces of the density were produced by tracing the gradient paths that originate at the bond critical points and following directions that are linear combinations of the vectors associated with the principal negative curvatures. Parameters describing the location of the critical points (r_A, r_B, F) and their values of the density and of its principal curvatures are listed in Table IV. Integrated charges of atoms and molecular fragments are summarized in Table V.

The topological characteristics of the N–N and C–N bonds reveal the same features that we have previously identified as typical for the diazonium function in general.[5,7,9] In all cases, the N_α basins extend greatly into the C–N bonding region (F_{CN} = 0.30) and modestly ($F_{N\alpha N\beta}$ = 0.56) into the N–N bonding region. Fairly constant ρ values of 0.22 and 0.68 are found for all of the C–N and N–N bond critical points. In Figure 3a, the charges determined for N_α, N_β, and the diazo groups are plotted using the cis preference energies (2 < 1 < 4) as the ordering principle. *Negative N_α charges* are found for all molecules; all fall within the range of –0.51 to –0.48. The N_α charges are smaller in magnitude in the cis than in the trans isomers, and importantly, the N_α charges in the cis isomers are decreasing with increasing nucleophilicity of the proximate oxygen atom whereas the N_α charges in the trans isomer are relatively unaffected. N_β charges are found in the range between +0.47 and +0.60 and they are larger for the cis than for the trans isomers. The charges of the individual N atoms show *large internal polarization of the N_2 groups in all cases and rather small overall charges.* The N_2 group charges are less than +0.10 in all cases, they decrease with the nucleophility of the proximate oxygen (Figure 3a), and for **4b** the N_2 group charge is even slightly negative.

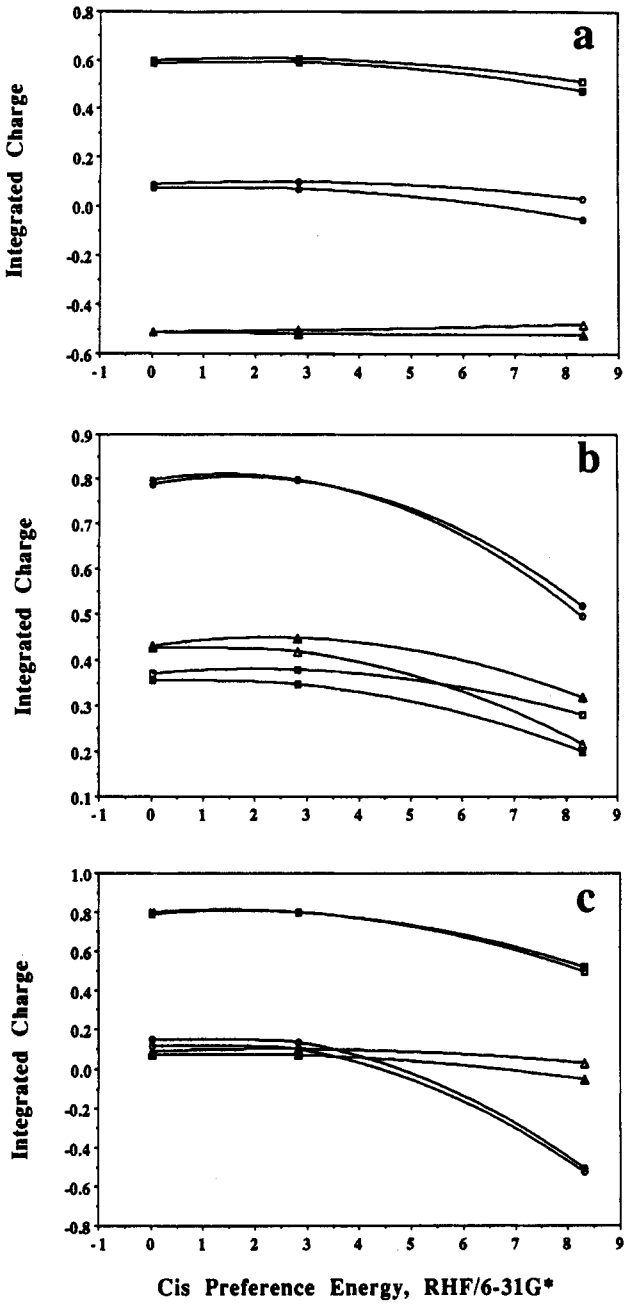

Figure 3. In plot a, the integrated charges of N_α (triangles), N_β (squares), and the diazo groups (circles) of **1**, **2**, and **4** are plotted versus their cis preference energies. Data related to the cis and trans isomers are represented with unfilled and filled marks, respectively. In plot b, the integrated charges of the C(1)H (triangles), the C(2)H (squares), and the C_2H_2 (circles) fragments are shown in a similar fashion. Plot c shows the dependence of the charges of the diazo function (triangles), the C_2H_2 fragments (squares), and the CO_2H or CO_2 groups.

In Figure 3b, the integrated charges of the C(1)H, the C(2)H, and the C_2H_2 fragments are shown. The C(1)H charges in the cis isomers are smaller than in the trans isomers while the opposite is true for the C(2)H charges and, usually, the C(1)H charges are larger than the C(2)H charges with the single exception of **4a**. The overall C_2H_2 charges show little dependency on CC configuration but depend greatly on the molecular charge. For ions **1** and **2**, C_2H_2 fragment charges are in the narrow range of +0.89 to +0.80, but they are much smaller for the overall neutral

(34) Structures **4** were also analyzed at the RHF/6-31+G* level, and very similar results were obtained. Topological properties of **4** and also of **5** at RHF/6-31+G* are given in the supplemental material.

Table IV. Topological Properties of the Electron Density Functions of Isomeric 3-Diazonium Propenoic Acids and of Isomeric 3-Diazonium Propenoate Zwitterions[a-f]

no.	A–B	r_A	r_B	F	ρ	λ_1	λ_2	λ_3	ϵ
				cis-3-Diazonium Propenoic Acid, **1a**					
1	C1–C2	0.598	0.724	0.452	0.365	−0.823	−0.589	0.144	0.398
2	C1–N3	0.439	0.996	0.306	0.215	−0.279	−0.270	1.101	0.032
3	N3–N4	0.598	0.476	0.557	0.683	−1.541	−1.539	0.444	0.002
4	C1–H5	0.730	0.341	0.681	0.296	−0.891	−0.848	0.472	0.050
5	C2–H6	0.725	0.350	0.674	0.295	−0.856	−0.853	0.481	0.004
6	C2–C7	0.777	0.732	0.515	0.276	−0.592	−0.559	0.319	0.057
7	C7–O8	0.387	0.796	0.327	0.445	−1.350	−1.191	3.028	0.134
8	C7–O9	0.416	0.885	0.320	0.339	−0.902	−0.892	1.686	0.012
9	O9–H10	0.785	0.173	0.820	0.346	−1.912	−1.889	1.654	0.012
10	ring	1.491	1.395	0.517	0.014	−0.011	0.026	0.072	
11	N3–O8	1.262	1.351	0.517	0.017	−0.016	−0.014	0.100	0.156
				cis-3-Diazonium Propenoic Acid, **2a**					
1	C1–C2	0.721	0.601	0.545	0.363	−0.816	−0.587	0.155	0.390
2	C1–N3	0.438	0.993	0.306	0.215	−0.272	−0.272	1.138	0.001
3	N3–N4	0.599	0.475	0.558	0.683	−1.544	−1.531	0.443	0.008
4	C1–H5	0.730	0.342	0.681	0.296	−0.888	−0.844	0.472	0.052
5	C2–H6	0.727	0.348	0.677	0.296	−0.863	−0.861	0.482	0.002
6	C2–C7	0.781	0.728	0.518	0.276	−0.589	−0.557	0.316	0.058
7	C7–O8	0.384	0.789	0.327	0.454	−1.398	−1.188	3.215	0.176
8	C7–O9	0.421	0.899	0.319	0.322	−0.829	−0.809	1.520	0.025
9	O9–H10	0.786	0.172	0.821	0.344	−1.907	−1.881	1.642	0.013
10	ring	1.521	1.386	0.523	0.012	−0.009	0.022	0.059	
11	N3–O8	1.289	1.367	0.485	0.015	−0.013	−0.012	0.088	0.103
				trans-3-Diazonium Propenoic Acid, **1b**					
1	C1–C2	0.721	0.600	0.546	0.366	−0.829	−0.595	0.150	0.394
2	C1–N3	0.436	0.993	0.305	0.214	−0.266	−0.260	1.180	0.212
3	N3–N4	0.599	0.476	0.557	0.682	−1.552	−1.523	0.451	0.019
4	C1–H5	0.740	0.333	0.690	0.295	−0.897	−0.856	0.468	0.047
5	C2–H6	0.721	0.354	0.671	0.294	−0.850	−0.843	0.480	0.008
6	C2–C7	0.790	0.726	0.521	0.273	−0.584	−0.551	0.318	0.060
7	C7–O8	0.386	0.793	0.327	0.449	−1.367	−1.191	3.090	0.148
8	C7–O9	0.417	0.888	0.320	0.335	−0.883	−0.874	1.639	0.010
9	O9–H10	0.784	0.173	0.819	0.347	−1.911	−1.888	1.654	0.012
				trans-3-Diazonium Propenoic Acid, **2b**					
1	C1–C2	0.721	0.600	0.546	0.365	−0.825	−0.594	0.153	0.388
2	C1–N3	0.437	0.995	0.305	0.212	−0.254	−0.254	1.156	0.000
3	N3–N4	0.599	0.477	0.556	0.682	−1.552	−1.522	0.453	0.020
4	C1–H5	0.736	0.336	0.687	0.296	−0.897	−0.855	0.469	0.049
5	C2–H6	0.722	0.352	0.672	0.295	−0.855	−0.850	0.481	0.006
6	C2–C7	0.788	0.722	0.522	0.275	−0.590	−0.556	0.316	0.061
7	C7–O8	0.385	0.790	0.327	0.452	−1.388	−1.187	3.176	0.169
8	C7–O9	0.420	0.894	0.319	0.327	−0.852	−0.838	1.556	0.015
9	O9–H10	0.785	0.173	0.820	0.346	−1.911	−1.886	1.650	0.013
				cis 3-Diazonium Propenoate Zwitterion, **4a**					
1	C1–C2	0.745	0.581	0.562	0.360	−0.785	−0.618	0.121	0.269
2	C1–N3	0.437	0.991	0.306	0.214	−0.281	−0.223	1.152	0.260
3	N3–N4	0.605	0.470	0.563	0.682	−1.521	−1.519	0.412	0.002
4	C1–H5	0.708	0.362	0.662	0.294	−0.852	−0.796	0.470	0.070
5	C2–H6	0.709	0.366	0.660	0.294	−0.843	−0.822	0.484	0.025
6	C2–C7	0.898	0.668	0.573	0.236	−0.471	−0.457	0.273	0.030
7	C7–O8	0.394	0.815	0.326	0.422	−1.250	−1.126	2.581	0.110
8	C7–O9	0.399	0.829	0.325	0.404	−1.172	−1.087	2.302	0.078
9	ring	1.406	1.383	0.504	0.018	−0.014	0.041	0.084	
10	N3–O8	1.171	1.284	0.477	0.025	−0.025	−0.024	0.149	0.051
				trans 3-Diazonium Propenoate Zwitterion, **4b**					
1	C1–C2	0.735	0.598	0.551	0.357	−0.778	−0.620	0.152	0.255
2	C1–N3	0.431	0.979	0.307	0.215	−0.263	−0.200	1.349	0.317
3	N3–N4	0.608	0.471	0.563	0.676	−1.537	−1.480	0.429	0.039
4	C1–H5	0.729	0.342	0.681	0.293	−0.877	−0.826	0.466	0.062
5	C2–H6	0.707	0.369	0.657	0.293	−0.837	−0.811	0.481	0.031
6	C2–C7	0.916	0.663	0.580	0.227	−0.445	−0.435	0.268	0.021
7	C7–O8	0.395	0.818	0.326	0.418	−1.234	−1.114	2.499	0.108
8	C7–O9	0.397	0.822	0.326	0.413	−1.208	−1.106	2.406	0.093

[a] At RHF/6-31G* for **1** and **2** and at RHF/3-31G*//RHF/6-31+G* for **4**. [b] r_A and r_B are the distances in angstroms between the critical point and the atoms A and B, respectively. F is defined as the ratio $r_A/(r_A + r_B)$. [c] The value of the electron density at the critical point, ρ, is given in e au^{-3}. [d] The curvatures of the electron density at the location of the critical points, λ_i, are given in e au^{-5}. [e] the ellipticity, ϵ, is defined as $\epsilon = \lambda_1/\lambda_2 - 1$. [f] These points are (3,−1) *ring* critical points. All other critical points are (3,+1) *bond* critical points.

zwitterions **4a** (+0.32) and **4b** (+0.52). In Figure 3c, the charges of the diazo function, the C_2H_2 fragments, and the CO_2H or CO_2 groups are shown. As to the ions **1** and **2**, the CO_2H groups are positively charged (+0.10 to +0.15) and somewhat more in the trans than in the cis isomers. Thus, the cations **1** and **2** are carbenium ions in which most

Table V. Integrated Properties of 3-Diazonium Propenoic Acid[a,b]

		cis-1a		*trans*-1b	
no.	atom	IC	$T = -E$	IC	$T = -E$
1	C1	+0.915	37.711 33	+0.190	37.727 51
2	C2	+0.188	37.830 33	+0.174	37.836 51
3	N3	−0.506	54.985 36	−0.520	54.988 53
4	N4	+0.604	53.937 43	+0.589	53.942 91
5	H5	+0.224	0.523 07	+0.258	0.506 09
6	H6	+0.191	0.538 07	+0.174	0.545 42
7	C7	+2.101	36.451 41	+2.122	36.440 87
8	O8	−1.367	75.732 04	−1.349	75.721 04
9	O9	−1.305	75.658 98	−1.307	75.652 44
10	H10	+0.670	0.301 71	+0.668	0.302 90
	Σ	+0.995	373.669 73	+0.999	373.664 22
			(0.000 29)		(0.001 30)
	N_2	+0.098	108.922 79	+0.069	108.931 44
	CO_2H	+0.099	188.144 14	+0.134	188.117 25
	C(1)H	+0.419	38.234 40	+0.448	38.233 60
	C(2)H	+0.379	38.368 40	+0.348	38.381 93
		cis-2a		*trans*-2b	
1	C1	+0.201	37.703 64	+0.183	37.728 56
2	C2	+0.174	37.838 36	+0.179	37.839 37
3	N3	−0.512	54.995 37	−0.514	54.983 22
4	N4	+0.599	53.940 41	+0.586	53.945 51
5	H5	+0.226	0.521 98	+0.247	0.512 51
6	H6	+0.196	0.536 47	+0.178	0.543 96
7	C7	+2.086	36.465 27	+2.118	36.453 78
8	O8	−1.312	75.717 03	−1.318	75.715 01
9	O9	−1.331[c]	75.746 43[c]	−1.320	75.643 98
10	H10	+0.673	0.298 60	+0.670	0.301 32
	Σ	+1.000	373.663 55	+1.009	373.667 22
					(0.003 24)
	N_2	+0.087	108.935 78	+0.072	108.928 73
	CO_2H	+0.116[c]	188.227 33[c]	+0.150	188.114 09
	C(1)H	+0.427	38.225 62	+0.430	38.241 07
	C(2)H	+0.370	38.374 83	+0.357	38.383 33
		cis-4a		*trans*-4b	
1	C1	+0.074	37.766 52	+0.097	37.767 67
2	C2	+0.165	37.850 36	+0.132	37.877 02
3	N3	−0.481	54.957 28	−0.526	54.986 74
4	N4	+0.511	53.983 02	+0.474	53.995 09
5	H5	+0.142	0.560 59	+0.222	0.521 49
6	H6	+0.115	0.572 33	+0.103	0.576 96
7	C7	+2.362	36.261 75	+2.381	36.240 04
8	O8	−1.424	75.664 08	−1.431	75.654 28
9	O9	−1.464	75.658 36	−1.455	75.649 04
	Σ	0.000	373.274 29	−0.003	373.268 33
			(0.002 78)		(0.007 06)
	N_2	+0.030	108.940 30	−0.052	108.981 83
	CO_2	−0.526	187.584 19	−0.505	187.543 36
	C(1)H	+0.216	38.327 11	+0.319	38.289 16
	C(2)H	+0.280	38.422 69	+0.200	38.344 63

[a] At RHF/6-31G* for 1 and 2 and at RFH/6-31G*//RHF/6-31+G* for 4. [b] IC is the integrated atom or fragment charge. The integrated atom and fragment kinetic energies are corrected for the virial defect of the wave functions and they are equal to the negative of the atom and fragment energies, $T = -E$. [c] By difference.

of the positive charge is located on the C_2H_2 fragments with only small positive charges on the attached (more electronegative) N_2 and COOH groups. Deprotonation of the acids leads to negative CO_2 group charges of −0.53 (**4a**) and −0.51 (**4b**) and about half of the negative charge is transferred (almost equally) to the CH groups of the C_2H_2 fragments.

The CO_2H groups in **1** and **2** are characterized by C charges of about +2.10, OH charges of −0.65, and carbonyl O charges of −1.32 to −1.33 (**2**) and −1.35 to −1.37 (**1**). It is significant for an argument to be made below that the negative charge of the carbonyl oxygen in **1a** is larger than the one in **2a**. Deprotonation of the acids increases the $C(CO_2)$ charge to +2.37 and the oxygen charges are increased to −1.42 and −1.46. Considering that the OH charges of −0.65 in the acids results from a typical O charge of −1.32 and a +0.67 H charge, the complete removal of the proton should merely increase the population of the remainder of the molecule by 0.33 electrons. This is accomplished by increases of the O charges by about 0.11, large increases of the C_2H_2 populations compared to the acids (vide supra), and a *charge increase* of the CO_2 carbon by 0.27. The polarity of the CO bonds is increased presumably to reduce electron–electron repulsion between the oxygens. We thus find that the removal of the proton has changed (*reduced*!) the overall population of the CO_2 group only very slightly (less than 0.05) and instead increased the population of the C_2H_2 fragment (about 0.28). This result suggests that the CO_2 fragment of the CO_2H group already is saturated with electrons in the acids and that a further stabilization of the CO_2 group cannot be accomplished by increasing its overall electron count. In fact, the fragment stabilities show that the CO_2 groups in **4a** and **4b** are greatly destabilized compared to the CO_2 groups in the acids; the CO_2 group in **4a** is 162.1 and 216.2 kcal/mol less stable than in **1a** and **2a** and the CO_2 group in **4b** is 170.1 and 169.1 kcal/mol less stable than the ones in **1b** and **2b**.

Nonbonded Distances in the Cis Isomers. A characteristic feature of the CNN skeletons in the cis isomers relates to their small deviation from linearity. This deviation can best be seen in **4a** where it is largest (8.9°) and it also occurs in **1a** and **2a** in the same direction but to a smaller extent (4.4°). It is primarily this feature together with the *formal* charge distribution indicated by the resonance form A that suggested an attractive electrostatic interaction between N_α and O_{pr}. The question then is whether this explanation is (a) consistent with the electronic structure of the diazonium ions and (b) whether it is the only consistent interpretation or whether there are other explanations that might fit the experimental and theoretical results just as well or even better.

The usually given explanation for the short N_α–O distance basically is an electrostatic argument and it relies on the assumption of a positive charge on N_α. This commonly accepted explanation cannot be correct because the electron density analysis of diazonium ions in general and of the systems studied here in particular (vide supra) clearly shows electron accumulation at N_α. In fact, we will show that the N_α–O_{pr} interaction is *repulsive* in nature. The analysis of the structures of the CC configurational isomers provides a first indication. We have pointed up above that the δ and the ϵ angles always are increased in going from the trans to the cis isomer. Minimization of the repulsive interaction between N_α and O_{pr} is a likely cause for this structural effect. Note that the N_α–O_{pr} distances in **1a**, **2a**, and in **4a** still remain shorter than 2.63 Å, a value that is significantly smaller than the sum of the van der Waals radii of N and O.[35] A slightly more involved electrostatic argument would have to consider not just N_α and O_{pr}, but also include the atoms N_β

	proximate oxygen, O_{pr}			carboxyl carbon		
	C(1)	N_α	N_β	C(1)	N_α	N_β
2a	2.851	2.626	3.016	2.553	3.010	3.752
1a	2.857	2.609	2.987	2.493	2.871	3.587
4a	2.770	2.454	2.877	2.557	2.895	3.644

and the carboxyl C. These four atoms are positioned in

(35) The van der Waals radii of (neutral) O and N are 1.4 and 1.5 Å, respectively. *CRC Handbook of Chemistry and Physics*, 66th ed.; CRC Press: Boca Raton, 1986, p D-166.

Chart V

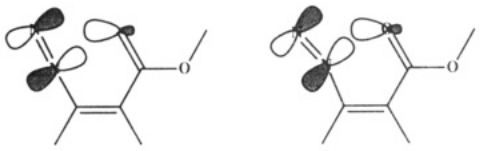

non-linear CNN

a quadrupolar arrangement with *nearly identical* N_α–C and N_β–O_{pr} distances; that is, two edges of the quadrupole are almost perfectly parallel. The structures may be regarded as those resulting from the optimization of this quadrupolar arrangement. This electrostatic model does not consider the short N_α–O_{pr} contact as the result of N_α–O_{pr} attraction but, instead, the short N_α–O_{pr} distances occur because of optimization of the N_β–O_{pr} and N_α–$C(O_{pr})$ interactions which overcompensate for the N_α–O_{pr} repulsion. The kink in the CNN skeleton can be explained in a straightforward fashion as the result of the interaction between the carbonyl C and N_α.

Molecular orbital overlap also might be a possible cause for the angular features of the cis-configured ions. The interaction between O_{pr} and N_α might be viewed as a donor–acceptor interaction between an O lone pair and the in-plane NN π^*-type MO. As is apparent from Chart V, such an interaction would nicely explain the nonlinearity of the CNN arrangement. The coefficient for the p-AO at N_α would be smaller than the one at N_β as a result of the internal polarization of the N_2 group, and thus the overlap would have to be reduced consequently. In any case, it appears unlikely that it is in fact an important interaction because any significant charge transfer associated with this type of interaction would result in a significant amount of electron density in the region between O_{pr} and N_α as well as an elongation of the NN bond. Neither of these features are manifested in the structures or in the electron densities. For example, the molecular graph of **1a** is shown in Figure 4 and there is indeed a bond path connecting N_α and the carbonyl oxygen, but the electron density at the "bond" critical point along this path is only 0.014 and only marginally higher than the ρ value at the ring critical point. The lack of substantial electron accumulation along the N_α–O_{pr} "bond" path is perfectly illustrated by the three-dimensional contour plot of the electron density of **4a** also shown in Figure 4. Considering the choice of the rather small contour setting, the plot demonstrates clearly that there is only a very small amount of electron density between N_α and O_{pr}. Equally small ρ values are found for the respective critical points in **2a** and **4a** (Table IV). The small ridge of electron density between the atoms N_α and O_{pr} more likely is the simple result of close geometric proximity and should not be taken as an indication of a "bond". The occurence of a bond path does not necessarily indicate a bonding interactions—repulsive interactions between atoms linked by a bond path are entirely possible.[36] This point of view also is supported by analysis of the electron-density difference functions.

Electron-Density Difference Functions. The analysis of electron-density difference functions serves as a powerful method for the examination of the postulated electron–electron repulsion effects between N_α and nucleophilic O_{pr} in the cis isomers. This analysis was carried out for **4a** and **4b** as the effects should be largest and best to identify in this case. Electron-density difference analysis

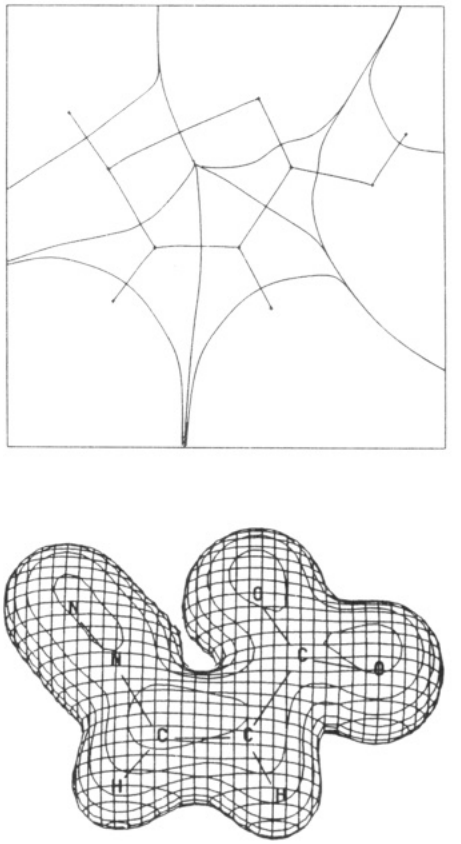

Figure 4. Bond paths together with the cross-sections of the zero-flux surfaces of the gradient of the electron density are shown for cis-3-diazonium propenoic acid **1a**. A "bond path" occurs between N_α and the proximate nucleophilic oxygen but the electron density in that region is *very* small. The three-dimensional contour plot of **4a** was produced with the rather low contour level of 0.03 e au^{-3} and it shows no N_α–O_{pr} bond.

requires that the fragments studied are superimposed with identical geometries and, when geometrical isomers are studied, one difference function needs to be examined for each of the fragments of interest. To study the electronic reorganization within the HCNN part of **4**, the electron densities of **4a** and **4b** were computed for structures in which the HCNN fragment and C(2) were placed at identical coordinates, their difference function $\Delta\rho' = \rho(cis\text{-}\mathbf{4a}) - \rho(trans\text{-}\mathbf{4b})$ was calculated, and contours of $\Delta\rho'$ (in the molecular plane) were determined and plotted to produce Figure 5. Similarly, the electronic reorganization within the CO_2 function was examined via the function $\Delta\rho'' = \rho(cis\text{-}\mathbf{4a}) - \rho(trans\text{-}\mathbf{4b})$ computed based on structures in which the atoms of the $HCCO_2$ group and C(1) were placed at identical positions (Figure 6). The functions $\Delta\rho'$ and $\Delta\rho''$ were determined with the smaller basis set and with the bond lengths and angles of **4b**. The structural parameters for **4a** and **4b** are rather similar, and they show little basis set dependency. The parameters of **4b** were used primarily because the δ angle in **4b** is smaller than in **4a** and, hence, possible features occurring in Figures 5 and 6 that are indicative of repulsive interactions between the N_2 and the COO groups might be regarded as the electronic origin of the driving force that leads to the larger δ angle in **4a**.

Figure 5 provides compelling evidence for the depletion of electron density at N_α in *cis*-**4a**. This finding supports our earlier argument based on N_α charges in the configurational isomers, but it goes beyond it since (a) the analysis of the $\Delta\rho$ functions is independent of the location of the zero-flux surfaces and (b) spacial information is retained.

(36) For a discussion of bond paths between the repulsive atoms in He dimer, see: R. Glaser, *J. Comput. Chem.*, submitted for publication.

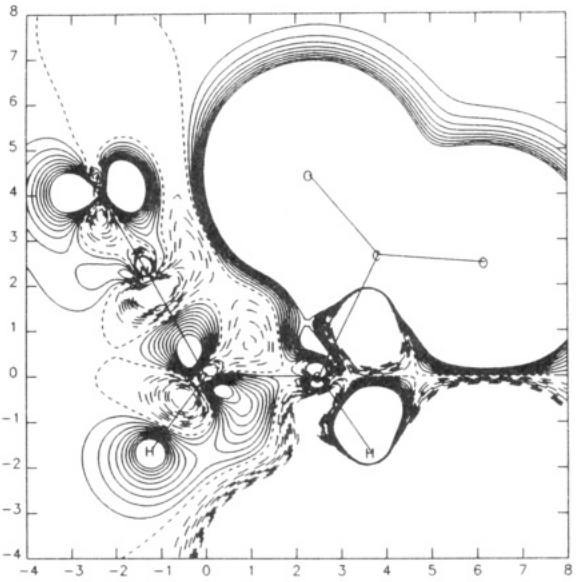

Figure 5. Effects of the proximate nucleophile on the electron density of the N_2 group. A contour plot is shown of the electron density difference function $\Delta\rho'$ obtained by subtraction of ρ(*trans*-**4b**) from ρ(*cis*-**4a**). Contour levels are from −0.01 to 0.01 e au^{-3} with a spacing of 0.001. Regions where $\Delta\rho' < 0$ and $\Delta\rho' > 0$ are contoured with dashed and solid lines, respectively, and the contour for which $\Delta\rho' = 0$ is drawn with short dashes.

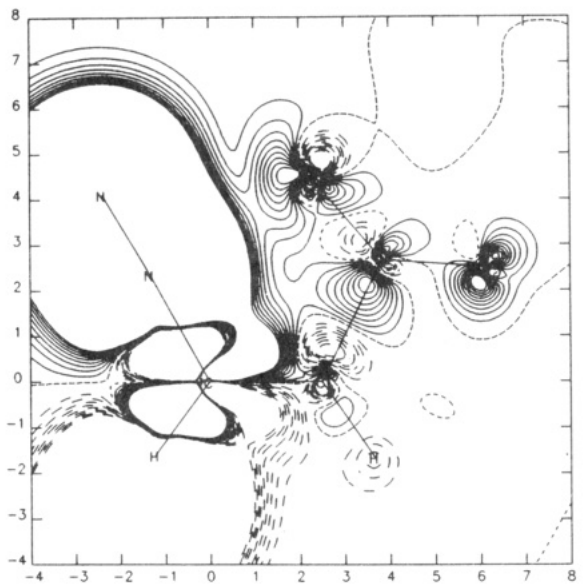

Figure 6. Effects of the proximate diazonium function on the electron density of the carboxylate group. A contour plot is shown of the electron density difference function $\Delta\rho''$ obtained by subtraction of ρ(*trans*-**4b**) from ρ(*cis*-**4a**). Contours are as in Figure 5.

The electron-density depletion occurs in the direction parallel to the CNN axis as well as perpendicular to it in the molecular plane. The overall reduction of the electron density in the in-plane π-type region of N_α is accompanied by a shift from the side facing O_{pr} to the other. The depletion at N_α primarily serves to increase the density at N_β, and this increase occurs in a π-type region that is perfectly aligned with the direction $N_\beta \rightarrow O_{pr}$. The anisotropy of the electron density in the C(1) basin significantly differs for **4a** and **4b**. In the C(1) basin of *cis*-**4a**, an electron-density increase occurs along the direction of the CN axis together with a depletion in the perpendicular direction (which closely coincides with the CH bond axis) compared to *trans*-**4b**. These changes might easily be

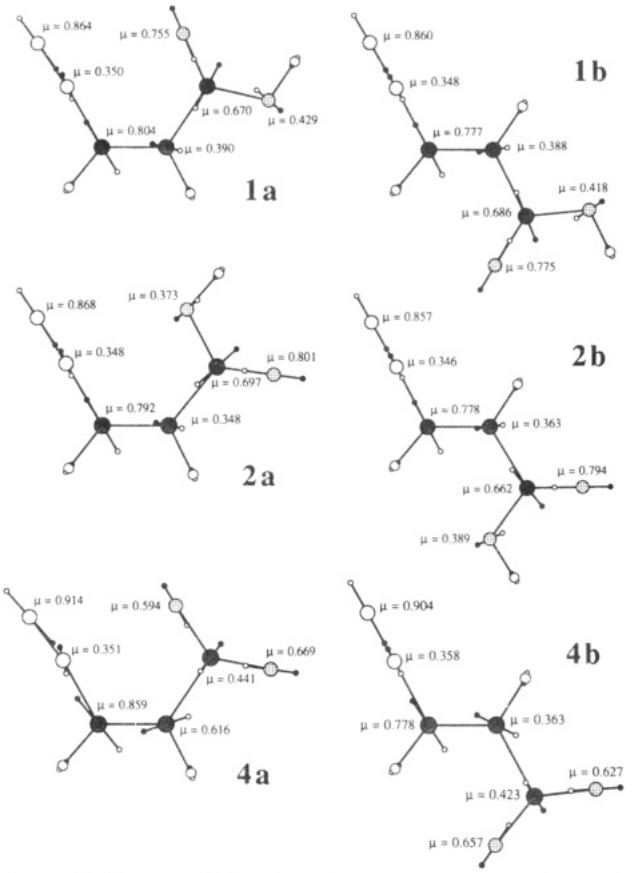

Figure 7. Integrated first electric moments are superimposed on the structure of **1**, **2**, and **4**. The atomic dipoles vectors μ are directed from the unfilled "o" to the filled black "o" markers. Note that the dipoles $\mu(N_\beta)$ and $\mu(O_{pr})$ are large and antiparallel to each other whereas the dipoles $\mu(N_\alpha)$ and $\mu(O_{pr})$ are parallel to each other.

interpreted as a response to the depletion in the N_α basin of **4a**. Probably the most significant feature of the function $\Delta\rho''$ relates to the spatial redistribution of the density in the O_{pr} basin. Figure 6 clearly shows that the O_{pr} density in **4a** is polarized in such a way as to direct its density in the best possible way toward N_β, not N_α.

Intramolecular Polarization, Atom Anisotropy, and Electrostatic Interactions. Chemists are prone to think of electronic structures in terms of atomic charges and to reflect on such charges with the implied assumption that discussions of charge distributions are correlated with energy considerations. While integrated atom and fragment energies do account for the electron density *distribution* within the basin, the determination of charges via density integration does not reflect the electron-density *distribution within the basin*. In order to recover the asymmetry of the electron-density function within each basin, the atomic moment μ requires consideration. The atomic moment μ is defined[37] as the negative of the volume integral of $\mathbf{r}'\,\rho(\mathbf{r})$ taken over the basin, where $\mathbf{r}'$ measures the distance of the position $\mathbf{r}$ from the position of the nucleus Y ($\mathbf{r}' = \mathbf{r} - \mathbf{Y}$). The μ vectors were determined, they are summarized in Table VI, and they are displayed in Figure 7. The μ vectors (o--o) are directed from the unfilled "o" to the filled black "o" markers.

In **1a**, the $\mu(N_\alpha)$ vector is directed toward N_β and $\mu(N_\beta)$ is antiparallel and much larger. These directions show that

(37) (a) Bader, R. F. W.; LaRouche, A.; Gatti, C.; Carroll, M. T.; MacDougall, P. J.; Wiberg, K. B. *J. Chem. Phys.* **1987**, *87*, 1142. (b) Slee, T. *J. Am. Chem. Soc.* **1986**, *108*, 7541.

Table VI. Atomic First Moments

	1a		2a		4a	
A–B	μ	angle	μ	angle	μ	angle
C1–N3	0.804	1.65	0.792	1.02	0.859	10.54
C2–C1	0.390	14.37	0.348	12.09	0.616	18.35
N3–N4	0.350	12.19	0.348	8.78	0.351	24.13
N4–N3	0.864	1.75	0.868	1.01	0.914	3.71
H5–C1	0.122	0.47	0.122	1.31	0.129	1.87
H6–C2	0.122	4.44	0.122	4.13	0.132	10.29
C7–C2	0.670	175.01	0.697	170.93	0.441	177.05
O8–C7	0.755	178.28	0.801	179.92	0.669	177.10
O9–C7	0.430	152.74	0.373	75.80	0.594	176.05
H10–O9	0.128	0.88	0.127	0.96		
	1b		**2b**		**4b**	
	μ	angle	μ	angle	μ	angle
C1–N3	0.777	0.11	0.778	0.84	0.755	5.54
C2–C1	0.388	8.59	0.363	7.39	0.573	26.85
N3–N4	0.348	0.58	0.346	0.87	0.358	1.41
N4–N3	0.860	0.01	0.857	0.05	0.904	0.15
H5–C1	0.121	4.30	0.120	4.45	0.128	8.65
H6–C2	0.123	7.55	0.123	7.61	0.135	13.89
C7–C2	0.686	175.92	0.662	171.89	0.423	175.48
O8–C7	0.775	178.69	0.794	179.78	0.657	176.88
O9–C7	0.418	152.78	0.389	151.88	0.627	175.44
H10–O9	0.128	0.91	0.128	0.88		

[a] Dipole moments are given in atomic units for atoms A. 1 au equals 2.5418 D. [b] The angles enclosed by the dipole moment of atom A and the bond direction A–B are given.

the electron density within the basins of N_α and N_β is polarized into the CN bonding and the lone-pair regions, respectively. The μ(C(1)) vector is directed toward N_α. All of these features are common to various diazonium ions.[38] Note that the μ directions may differ substantially from the geometrical bond directions. The μ vectors associated with the CNN fragment in **1a** are nearly parallel with bond directions, but the deviations become as large as 25° in **2a** and **4a**. While the topological properties and the integrated charges indicate but small differences in the N_α basins of **1a**, **2a**, and **4a**, the μ vectors clearly show the significant effects of the proximate nucleophiles on the anisotropic electron distributions within the N_α basins reflecting the density redistribution shown by the $\Delta\rho$ functions. The atoms of the carboxyl groups are assigned rather large charges and the (large) dipole moments of the atoms indicate atomic polarizations that counteract. The μ vectors of the carboxyl carbons all are more or less parallel to the C–CO_2 bond and directed into the region between the oxygens, and the μ vectors of carbonyl and carboxylate oxygens are all directed toward the carboxyl carbon. The hydroxyl oxygens in **1a**, **1b**, and **2b** have μ vectors that are nearly perpendicular with and directed away from the C–CO_2 axes, but a neighboring group effect on the μ vectors of the hydroxyl group in **2a** is evident.

Arguments based on atomic charges and dipole moments become rather involved as many values and directions need to be considered, and the inclusion of higher moments complicates matters even more. It is therefore important to define and discuss appropriate parameters that incorporate all of this information in a proper fashion. As the basis for such parameters, we consider the electrostatic interaction energy between atoms i and j, ESI_{ij}, defined by the equation

$$ESI_{ij} = CC_{ij} + CD_{ij} + DD_{ij} + QC_{ij} + QD_{ij} + QQ_{ij}$$

where CC_{ij} is the Coulomb energy between the integrated atomic charges q_i and q_j, CD_{ij} is the sum of the energies

(38) See refs 5 and 7.

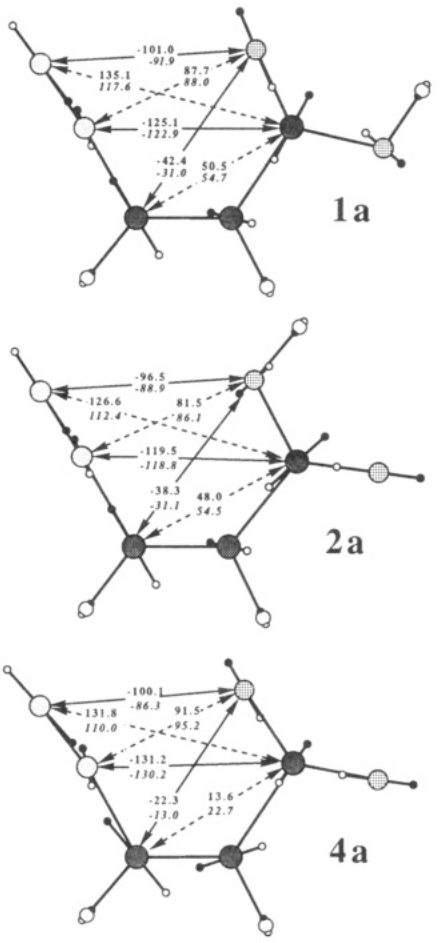

Figure 8. Electrostatic interaction energies ESI_{ij} (in kcal/mol) between pertinent pairs of atoms are shown for the *cis*-configured 3-diazonium propenoic acid **1a** (top) and **2a** (center) and the zwitterion **4a**. Solid (dashed) arrows and negative (positive) interaction energies indicate attraction (repulsion). Values given in italics are the Coulomb components CC_{ij} of ESI_{ij}.

associated with the interaction of q_i with μ_j and of q_j with μ_i, and DD_{ij} is the energy of interaction between the μ vectors i and j. To explore the importance of contributions involving higher-order atomic moments, we have also considered the interactions of the integrated atomic quadrupoles with the charges (QC_{ij}), dipoles (QD_{ij}) and quadrupoles (QQ_{ij}). We have determined all of these interaction terms for all of the minima. As an example, the results obtained for **1a** are listed in Table VII in matrix form. The electrostatic interaction matrices for the other molecules are given as supplementary material. For each pair of atoms in **1a**, the electrostatic contributions associated with CC_{ij}, CD_{ij}, DD_{ij}, QC_{ij}, QD_{ij}, and QQ_{ij} interactions are listed together with their sum $\sum = ESI_{ij}$. Usually the CC_{ij} term is dominant, followed by the CD_{ij} term, and with few exceptions the DD_{ij} terms are much smaller. The electrostatic terms associated with the quadrupoles usually are small with the exception of those terms that involve bonded atoms.

The ESI_{ij} values greatly aid in the analysis of the neighboring group interactions between the diazonium group and the carboxy group in the cis isomers. These ESI_{ij} values are shown in Figure 8; solid arrows indicate electrostatic attraction (negative values) and dashed arrows show electrostatic repulsion. The two numbers given for each of the pairwise interactions are the ESI_{ij} values (C, D, and Q) and its Coulomb component alone (C, in italics) in kilocalories per mole. It is evident that the terms CD_{ij} and DD_{ij} are nonnegligible while those involving the

Table VII. Electrostatic Interaction Matrix for *cis*-3-Diazonium Propenoic Acid 1a[a,b]

		C2	N3	N4	H5	H6	C7	O8	O9	H10
CC	C1	9.2	-22.9	15.6	13.6	6.0	54.7	-31.0	-23.8	10.0
CD		-0.6	-40.5	18.3	-5.5	-4.8	-4.3	-10.9	3.3	-0.5
CQ		-6.4	10.2	-3.0	-4.6	-1.4	-2.2	1.2	0.6	-0.1
DD		-6.5	-8.8	4.1	-2.4	-0.7	0.1	-0.5	0.1	0.0
DQ		-2.7	-2.5	3.3	0.5	0.2	-0.4	-0.2	-0.1	0.0
QQ		3.2	2.1	0.2	0.9	0.1	0.0	0.0	0.0	0.0
Σ		-3.7	-62.3	38.5	2.4	-0.5	47.9	-41.4	-19.9	9.4
CC	C2		-13.2	11.1	6.5	11.1	87.0	-36.3	-35.2	13.2
CD			-7.5	5.7	3.4	-4.1	-30.4	-5.7	11.8	-2.6
CQ			0.9	-0.5	-0.9	-2.7	-9.7	0.4	3.6	-0.7
DD			-0.7	0.7	0.3	-2.4	2.3	-0.2	0.4	-0.1
DQ			-0.1	0.4	0.4	-0.9	-3.1	-0.1	-0.6	0.1
QQ			0.1	0.0	0.0	0.5	-0.1	0.0	0.1	0.0
Σ			-20.6	17.3	9.7	1.6	45.9	-41.9	-20.0	9.8
CC	N3			-94.5	-18.2	-9.6	-122.9	88.0	52.8	-23.9
CD				-35.0	-4.9	-1.8	-2.4	-0.3	3.8	-0.8
CQ				1.6	-0.1	0.0	-0.2	0.0	0.2	0.0
DD				22.2	-0.3	-0.1	0.2	0.0	0.1	0.0
DQ				33.9	0.0	0.0	-0.1	0.0	0.0	0.0
QQ				3.9	0.0	0.0	0.0	0.0	0.0	0.0
Σ				-67.8	-23.5	-11.5	-125.4	87.7	56.9	-24.7
CC	N4				14.8	8.7	117.6	-91.9	-53.6	25.4
CD					4.2	2.1	17.7	-9.5	-8.1	2.6
CQ					-0.2	-0.1	-0.9	-0.1	0.1	0.0
DD					0.2	0.1	-0.2	0.4	-0.2	0.0
DQ					0.1	0.0	0.1	0.0	0.0	0.0
QQ					0.0	0.0	0.0	0.0	0.0	0.0
Σ					19.1	10.8	134.3	-101.1	-61.8	28.0
CC	H5					5.7	44.5	-25.9	-21.7	9.4
CD						0.7	1.6	-2.9	-1.6	0.6
CQ						0.0	-0.3	0.1	0.0	0.0
DD						0.0	-0.2	-0.1	0.0	0.0
DQ						0.0	0.0	0.0	0.0	0.0
QQ						0.0	0.0	0.0	0.0	0.0
Σ						6.4	45.6	-28.8	-23.3	10.0
CC	H6						59.5	-26.4	-33.0	12.2
CD							3.4	-4.7	-2.0	0.9
CQ							-0.7	0.2	-0.3	0.0
DD							-0.5	-0.2	0.0	0.0
DQ							-0.1	0.0	0.0	0.0
QQ							0.0	0.0	0.0	0.0
Σ							61.6	-31.2	-35.3	13.1
CC	C7							-806.3	-700.5	249.3
CD								-267.3	-108.3	26.0
CQ								16.3	10.0	-0.6
DD								-16.8	-3.0	0.6
DQ								-13.6	-4.9	0.1
QQ								0.2	0.3	0.0
Σ								-1087.5	-806.2	275.4
CC	O8								265.8	-128.2
CD									51.2	-11.5
CQ									0.2	-0.2
DD									2.4	-0.1
DQ									0.0	0.0
QQ									0.0	0.0
Σ									319.5	-140.0
CC	O9									-303.1
CD										-37.6
CQ										-13.6
DD										-0.6
DQ										4.0
QQ										-0.1
Σ										-351.1

[a] Based on integrated charges and dipoles determined with the RHF/6-31G*//RHF/6-31G* wave function. [b] All values are in kcal/mol.

quadrupoles are negligible. Most importantly, this analysis provides compelling evidence that *the interaction between N_α and the proximate oxygen is repulsive in nature.* Strong attractive electrostatic interactions are found between N_α and the carboxyl C and between the N_β and O_{pr}, and a substantial repulsion occurs between N_β and the carboxyl C. An important result of the electronic structure analysis above relates to the reduction of charge on the C_2H_2 fragments upon deprotonation. As a consequence, the consideration of the C atom to which the N_2 group is

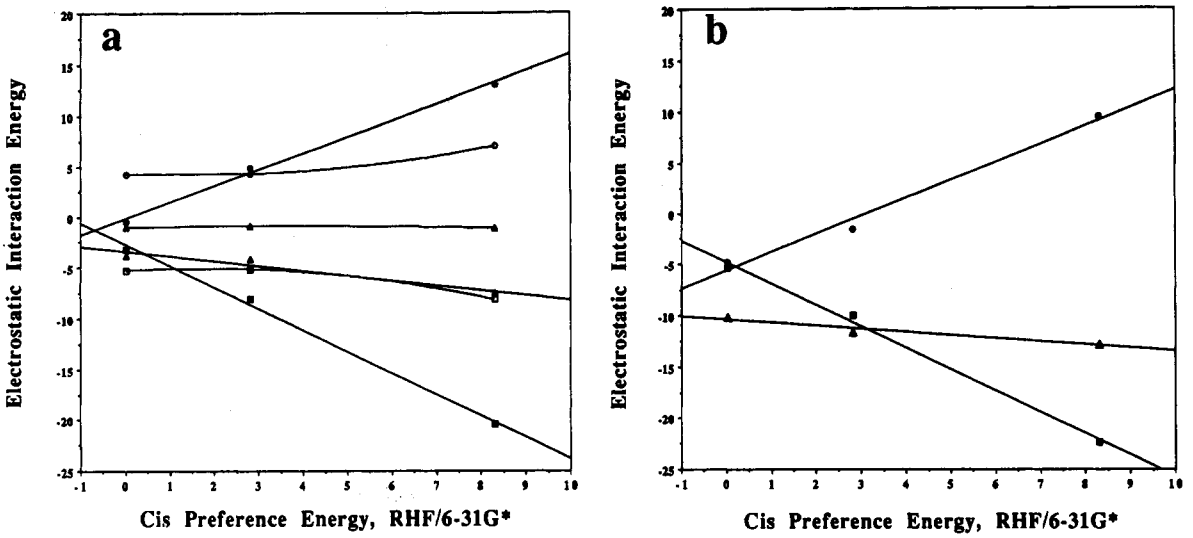

Figure 9. Electrostatic neighboring group interactions NGI_{cis} (squares), NGI_{trans} (triangles), and ΔNGI (circles) determined with method 2 (solid) are plotted versus the cis preference energies of 1, 2, and 4. Plot a shows interaction energies determined with atomic charges and dipoles, and plot b includes atomic quadrupoles. The unfilled marks in plot a show results obtained with method 1.

Table VIII. Electrostatic Neighboring Group Interactions[a]

		method 1			method 2		
terms[b,c]	no.	NGI_{cis}	NGI_{trans}	ΔNGI	NGI_{cis}	NGI_{trans}	ΔNGI
C,D	1	−5.19	−0.99	4.20	−8.06	−4.23	4.83
C,D	2	−5.29	−1.09	4.20	−3.27	−3.82	−0.55
C,D	4	−8.22	−1.26	6.96	−20.53	−7.58	12.95
C,D,Q	1	−6.03	−1.71	4.32	−10.04	−11.64	−1.61
C,D,Q	2	−6.16	−1.73	4.42	−5.33	−10.15	−4.82
C,D,Q	4	−8.94	−1.74	7.20	−22.42	−12.83	9.59

[a] Values are in kcal/mol. See text for definition of terms. [b] Regressions for C,D results: $NGI_{cis} = -2.111CPE_{RHF} - 2.769$ (R^2 = 0.996); $NGI_{trans} = -0.476CPE_{RHF} - 3.440$ (R^2 = 0.944); $\Delta NGI = 1.609CPE_{RHF} - 0.243$ (R^2 = 0.995). [c] Regressions for C,D,Q results: $NGI_{cis} = -2.091CPE_{RHF} - 4.820$ (R^2 = 0.995); $NGI_{trans} = -0.309CPE_{RHF} - 10.391$ (R^2 = 0.938); $\Delta NGI = 1.782CPE_{RHF} - 5.576$ (R^2 = 0.985).

attached becomes pertinent. Figure 8 shows that the C(1) is attracted to O_{pr} and repelled by the carboxyl C and that the combined interaction is overall repulsive in 1 and 2 but attractive in the zwitterion 4. In all cases, the close approach of O_{pr} to N_α is *a consequence but not the origin* of placing O_{pr} in the best possible bridging position between N_β and the C(1) carbon atom.

In order to compare the overall electrostatic interaction between the neighboring groups, we define the ESI value of a fragment, ESI^f, as the sum of all pairwise ESI_{ij} interactions between its atoms. The neighbor group interaction (NGI) between groups k and l then results as the difference between the $ESI^f(k)$ and $ESI^f(l)$ values of the neighboring groups and the $ESI^f(k+1)$ value computed with the atoms of both fragments. The NGI values have been determined for the cis isomers, NGI_{cis}, and for the trans isomers, NGI_{trans}, in two ways. In both cases, all of the atoms of the carboxyl group were included in one fragment and the other fragment either included just N_α and N_β (method 1) or the N_2 group and C(1) as well (method 2). Results are summarized in Table VIII and graphically depicted in Figure 9 with consideraton of charges and dipoles only (plot a) and with the quadrupoles included (plot b). The parameter ΔNGI is the difference $NGI_{trans} - NGI_{cis}$ and reflects the cis preference of the neighboring groups. In Figure 9a, NGI_{cis}, NGI_{trans}, and ΔNGI determined with and without consideration of C(1) are plotted versus the cis preference energies of 1, 2, and 4. Good correlations between the cis preference energies (CPE) and the NGI values are obtained when the C(1) carbon is considered. This result points up that the deprotonation of the carboxyl group not only affects the electronic structure of the carboxyl group but has significant effects on the C atom to which the diazo group is attached. *The through-space interaction of the neighboring groups is greatly affected by the through-bond electronic effects.* The linear correlations (Table VIII) between ΔNGI and CPE yield similar slopes (1.6 and 1.8) but different non-zero intercepts. Qualitatively, it is clear that the interaction of C(2) with both fragments contributes repulsive terms that would increase the intercept and possibly reduce the slope, but the electrostatic model cannot be expected to reproduce these contributions quantitatively because the assumption of point charges and point moments is certainly unwarranted if interactions are considered between atoms that are within their covalent bonding distances. It is important to note that in the definition of the NGI values, no such terms occur. The differences between plots a and b in Figure 9 are mostly caused by the lowering of the NGI_{trans} values when quadrupoles are included. Primarily, the interactions between C1 and the proximate CO bond are responsible for these shifts. Considering the decrease of NGI_{cis} and the relative constancy of NGI_{trans} with the increase of the CPE values, we can conclude that the cis preference energies are indeed caused by the differences in the through space interactions of the neighboring groups in the cis isomers.

Conclusion

The explanation of distortions in the crystal structure of diazonium ions by "incipient nucleophilic attack at N_α" relies on the assumption that N_α carriers a positive charge and thus implies that the electronic structure of diazonium ions is well represented by the Lewis structure. We have argued that this commonly accepted assumption is inconsistent with the analysis of the diazonium propenoic acid model systems. Since all of the diazonium ions that we have studied do have rather typical common structural and electronic features,[5,7,9,10] it appears reasonable to assume that our findings carry over to the larger molecules and, hence, that the explanation for the distortions in the crystal structures requires revision in general. Our new bonding model is based directly on the electron densities, and we have shown that this bonding model allows for a

consistent explanation of the structural features found in crystal structures of diazonium ions with proximate nucleophiles and, thus, we have provided *a crucial link between our theoretically derived bonding model and experimental data.*

Specifically, the presented analysis shows that distortions occur in order to optimize the electrostatic interactions associated with the quadrupolar charge arrangement on the atoms of the N_2 group and the proximate C–O_{pr} bond in the cis isomers. The close approach of the proximate nucleophile to the diazonium group occurs *despite* N_α–O_{pr} *repulsion.* The analysis points up the importance of neighboring group interactions involving the C atom to which the diazo group is attached and emphasizes the O_{pr} bridging position relative to this C and N_β. Our explanation is consistent with structural differences in the configurational isomers, the integrated populations, and with the electronic effects of neighboring group interactions as evidenced by the electron density difference function analysis of geometrical isomers.

A new method has been described for the evaluation of neighboring group interactions based on atomic charges, first moments, and quadrupoles. The role of the atomic first moments for a correct appreciation of the anisotropy of the electron density distribution within the atomic basins has been emphasized and numerical evidence indicates that their consideration is crucial for an adequate description of electrostatic interaction between neighboring groups. Linear correlations are found between the electrostatic interactions of the neighboring groups in the cis isomers and the O_{pr} nucleophilicity as well as between the differences in these electrostatic interactions in geometrical isomers and the cis preference energies. We conclude that the cis preference energies are indeed the result of through space electrostatic interactions in the cis isomers. The described method for the examination of neighboring group interactions on the basis of integrated atomic charges and dipoles should prove generally valuable for studies of this kind.

Acknowledgment. This work was supported by a National Institutes of Health Institutional Biomedical Research Support Grant (No. RR 07053). Acknowledgment is made to the donors of the Petroleum Research Fund, administered by the American Chemical Society, for partial support of this research. R.G. gratefully acknowledges financial support by a UMC Summer Research Fellowship. M.K.H. was supported by a Howard Hughes Undergraduate Research Fellowship and by a Monsanto Fellowship. We thank the Campus Computing Center for generous grants of computer time on the IBM 3090 and 4381 mainframes as well as on the attached FPS array processor.

Note Added in Proof. After acceptance of this paper, we have been able to determine the crystal structures of the precursor for benzyne formation, 2-carboxybenzenediazonium zwitterion, of its conjugate acid, 2-diazonium benzoic acid, and of their 1:1 complex. For all of these structures, we have found that (a) the diazonium group and the carboxyl group are on opposite sides of the (best) plane of the benzene ring and (b) most importantly that the carboxyl groups are rotated around the C–C(O_2) axis in such a way as to increase the N_α–O_{pr} distance. For example, the carboxylato group in the zwitterion is rotated by 26°. These experimental results provide strong evidence in support of the analysis presented here.

Registry No. 3-Diazonium propenoic acid, 137433-93-3; 3-diazonium propenoate, 137433-94-4.

Supplementary Material Available: Total energies and vibrational zero-point energies, topological and integrated properties of **3b**, **4**, and **5**, and electrostatic interaction matrices for **1b**, **2a**, **2b**, **4a**, and **4b** (12 pages). This material is contained in many libraries on microfiche, immediately follows this article in the microfilm version of the journal, and can be ordered from the ACS; see any current masthead page for ordering information. The supplementary material can be obtained from the authors via electronic mail (CHEMRG at UMCVMB).